

Mapping the Ultrafast Dynamics of Adenine onto Its Nucleotide and Oligonucleotides by Time-Resolved Photoelectron Imaging

Adam S. Chatterley,^{†,‡,§} Christopher W. West,[†] Gareth M. Roberts,^{‡,⊥} Vasilios G. Stavros,[‡] and Jan R. R. Verlet^{*,†}

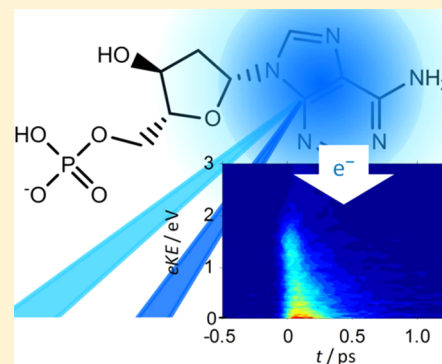
[†]Department of Chemistry, University of Durham, Durham DH1 3LE, United Kingdom

[‡]Department of Chemistry, University of Warwick, Coventry CV4 7AL, United Kingdom

S Supporting Information

ABSTRACT: The intrinsic photophysics of nucleobases and nucleotides following UV absorption presents a key reductionist step toward understanding the complex photodamage mechanisms occurring in DNA. The decay mechanism of adenine in particular has been the focus of intense investigation, as has how these correlate to those of its more biologically relevant nucleotide and oligonucleotides in aqueous solution. Here, we report on time-resolved photoelectron imaging of the deprotonated 3'-deoxy-adenosine-5'-monophosphate nucleotide and the adenosine di- and trinucleotides. Through a comparison of gas- and solution-phase experiments and available theoretical studies, the dynamics of the base are shown to be relatively insensitive to the surrounding environment. The decay mechanism primarily involves internal conversion from the initially populated $^1\pi\pi^*$ states to the ground state. The relaxation dynamics of the adenosine oligonucleotides are similar to those of the nucleobase, in contrast to the aqueous oligonucleotides, where a fraction of the ensemble forms long-lived excimer states.

SECTION: Biophysical Chemistry and Biomolecules



The absorption of ultraviolet (UV) radiation by DNA can lead to biological damage, including strand breaks and mutations that can ultimately lead to photolesions, transcription errors, and cancer.¹ Despite the efficient UV absorption, mediated by the optically bright $^1\pi\pi^*$ states localized on the four DNA nucleobases, the photodamage quantum yield in DNA is low (<1%).^{2,3} This photostability is governed by the nonradiative decay mechanisms that enable the nucleobases to assimilate and dispose of the potentially harmful electronic energy in a nondestructive fashion. Gaining a molecular-level understanding of these processes has been a long-standing goal, not only because of its role in radiation damage of DNA but also to assess why nature has evolved using such a select number of molecular building blocks to define the genetic code.⁴

Much of the experimental effort has been devoted to the fate of adenine (Ade) following excitation to its $^1\pi\pi^*$ states. Gas-phase spectroscopy^{5–11} synergized with theoretical calculations^{12–17} in particular has provided deep insight. However, there remains disagreement about the basic radiationless decay mechanism and, in particular, how the dynamics of Ade relate to those of its more biologically relevant nucleotide and oligonucleotides in aqueous solution. Although ultrafast spectroscopy on aqueous-phase nucleotides probes the more relevant environments, such experiments generally come at the cost of the detail that can be attained through the gas phase. In order to bridge the gap between the isolated Ade base and solvated nucleotides, we have performed experiments on the

isolated nucleotide. Specifically, we use electrospray ionization (ESI) to generate deprotonated 3'-deoxy-adenosine-5'-monophosphate (dAMP[−], Figure 1a) and employ time-resolved photoelectron imaging as a means of probing the dynamics of the *neutral* Ade nucleobase in this environment. Our results enable a comparison between previous studies carried out in the gas and in solution phases as well as with the extensive theoretical studies. This body of data allows the influence of the environment on the excited-state dynamics to be probed and provides insights into the most likely decay mechanism.

A key result is that the dynamics of Ade appear to correlate closely with those of its nucleotide, regardless of whether it is solvated or not. This is in agreement with some theoretical predictions and suggestions that the excited-state dynamics proceed primarily on a single excited state.^{14,18–20} But how do the base dynamics extend to larger oligomeric systems? In aqueous solution, new mechanisms become accessible, which occur alongside apparently monomeric dynamics.^{2,3} Although these competing processes have attracted much recent attention, their dynamics can obscure those due to single bases in the nucleotide, which is at the heart of understanding how the base dynamics evolve with size and remains one of the most important photoprotection mechanisms in DNA.²¹ In

Received: February 7, 2014

Accepted: February 11, 2014

Published: February 11, 2014

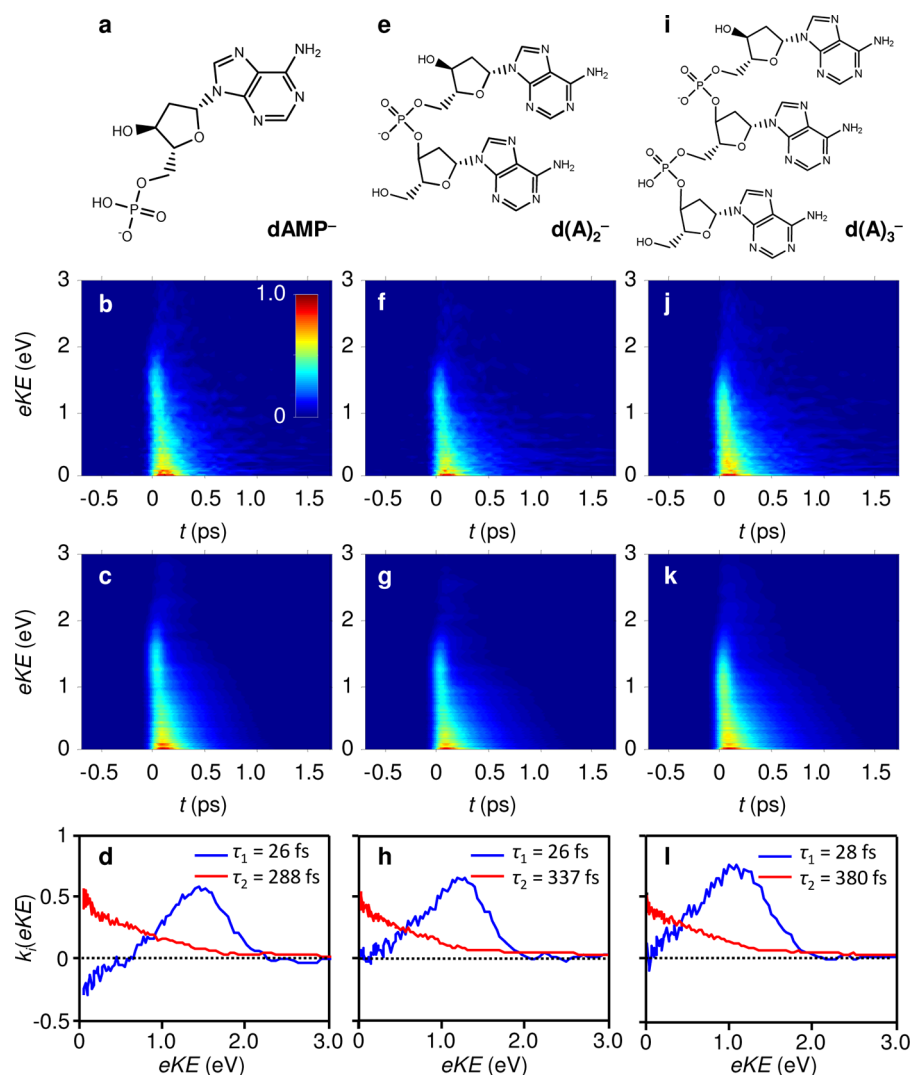


Figure 1. Time-resolved photoelectron spectra of dAMP⁻, d(A)₂⁻, and d(A)₃⁻. (a) Chemical structure of dAMP⁻. (b) False color representation of the time-resolved photoelectron spectra of dAMP⁻ excited at 4.66 eV and probed at 3.10 eV. (c) Global fit to the experimental data in (b), modeled with two exponential decay functions (see text). (d) Decay-associated spectra from the global fit in (c), showing the spectra of the two decay processes with associated lifetimes indicated. Panels (e–h) and (i–l) show the same as (a–d) but for d(A)₂⁻ and d(A)₃⁻, respectively.

order to explore this evolution, we have also extended our studies to isolated adenosine di- and trinucleotides.

Experiments were conducted using our femtosecond anion photoelectron imaging spectrometer, which has been described in detail previously,^{22–24} and combines ESI with velocity map imaging.²⁵ dAMP⁻ anions were produced by ESI at -2.5 kV from a ~ 1 mM solution of a dAMP sodium salt (98% Sigma-Aldrich) in methanol, and oligonucleotide anions were produced by ESI from a ~ 0.5 mM solution of the oligonucleotide (desalted, Sigma-Aldrich) in methanol. The anions were transferred into vacuum and accumulated in a ring electrode ion trap, and packets were ejected at a 50 Hz repetition rate into a collinear time-of-flight mass spectrometer. The mass-selected ion packet was intersected in the center of a velocity map imaging setup by femtosecond pump and probe laser pulses. Detached photoelectrons were directed onto a position-sensitive detector, and photoelectron images were typically collected for 5×10^4 laser shots per pump–probe delay. For each delay, a photoelectron image acquired for an equal number of laser shots without ions was subtracted to remove background photoelectron noise induced by the 266

nm light. Raw images were deconvoluted using the polar onion-peeling algorithm.²⁶ The energy resolution is $\Delta eKE/eKE \approx 5\%$, and spectra have been calibrated to the well-known spectrum of iodide.

Femtosecond laser pulses were derived from a commercial Ti:Sapphire oscillator and amplifier laser, centered at 1.55 eV (800 nm). The 4.66 eV (266 nm) pump pulses were generated using two type I β -barium borate (BBO) crystals, first to produce 3.10 eV (400 nm) light using second harmonic generation followed by sum frequency generation to mix the 3.10 eV photons with the 1.55 eV fundamental. The 3.10 eV (400 nm) probe pulses were generated using a further type I BBO crystal. Probe pulses were delayed with respect to the pump using a motorized optical delay line. Pump and probe beams were combined collinearly using a dichroic mirror and loosely focused into the interaction region with a curved mirror. The intensity of both beams was below 10^{11} W cm⁻². The cross-correlation of the pump and probe pulses was approximately 120 fs, providing a temporal resolution of ~ 60 fs.

To support our measurements, density functional theory (DFT) and time-dependent DFT (TD-DFT) calculations on

both nucleotide anions and nucleobases (as well as Ade-9Me) were performed using the PBE0 functional²⁷ in the Gaussian09 computational suite.²⁸ The functional has been selected for its balanced and robust description of both valence and Rydberg excited states in TD-DFT calculations.²⁹ All vertical excitation energies were calculated at the PBE0/aug-cc-pVDZ//TD-PBE0/aug-cc-pVTZ level of theory. Optimized ground-state geometries were confirmed to be (local) minima, as verified through further harmonic frequency calculations (no imaginary frequencies). The effects of a water solvent were simulated using a polarizable continuum model (PCM).

Time-resolved photoelectron spectra for dAMP[−] are shown as a false color plot in Figure 1b. In this, the two-photon contribution from the pump only has been subtracted, which recovers the pump–probe excited-state signal because the probe is not resonant with any initial transition. An increase in photoelectron yield at $t = 0$ is observed as population is transferred to the $^1\pi\pi^*$ states by the pump. Inspection of the spectra shows two dominant features; at electron kinetic energies $eKE < 0.7$ eV, there is a component that decays over the course of hundreds of femtoseconds, while within $1 < eKE < 2$ eV, a feature decays within the instrument response.

Quantitative insight can be gained by employing a global fitting procedure,³⁰ whereby the time-resolved photoelectron spectra, $S(eKE, t)$, are fit simultaneously in energy and time by the following equation

$$S(eKE, t) = \sum_i k_i(eKE) \left[\exp\left(\frac{-t}{\tau_i}\right) * g(t) \right]$$

where $k_i(eKE)$ is the decay-associated spectrum with the i th spectral feature that is decaying exponentially with a lifetime τ_i . The instrument response function was represented by a Gaussian, $g(t)$. Support plane analysis was used to estimate confidence intervals at the 95% level, and the greater of the upper and lower bounds has been reported as the error.

The results of the global fit are shown in Figure 1c. Only two exponential functions with lifetimes $\tau_1 < 60$ fs and $\tau_2 = 290 \pm 50$ fs are required to fully recover the data (residuals are shown in Figure S1, Supporting Information); the corresponding decay-associated spectra are shown in Figure 1d. Actual τ_1 lifetimes obtained from the fit are shown in Figure 1 but are limited by our time resolution of ~ 60 fs. The spectrum of the fast decay, $k_1(eKE)$, shows a peak within $0.7 < eKE < 2$ eV but is negative for $eKE < 0.5$ eV. Negative signals point to a concomitant exponential rise with a time constant of τ_1 ; thus, signal that was initially contributing to the $0.7 < eKE < 2$ eV feature is decaying into a feature at $eKE < 0.5$ eV. The dynamics are sequential, and the initial spectral peak around $0.7 < eKE < 2$ eV decays to form the decay-associated spectrum $k_2(eKE)$, which subsequently decays on a time scale of $\tau_2 = 290$ fs.

The time-resolved photoelectron spectroscopy following excitation at 4.66 eV of Ade and a derivative, Ade-9Me (in which the H atom at the N9 position has been methylated; see Figure 2), has been performed by Stolow and co-workers, and the analysis used was as done here.^{5,7,8} Their study had shown that the dissociative $^1\pi\sigma^*$ state, which is localized on the N9–H bond, may be involved in the decay dynamics of Ade but not Ade-9Me. This was discerned from the shape of the decay-associated spectra, which showed additional features due to the $^1\pi\sigma^*$ state. Comparison of the decay-associated spectra for dAMP[−] (Figure 1d) with those of Ade-9Me (see Figure S3, Supporting Information) shows striking similarities with the

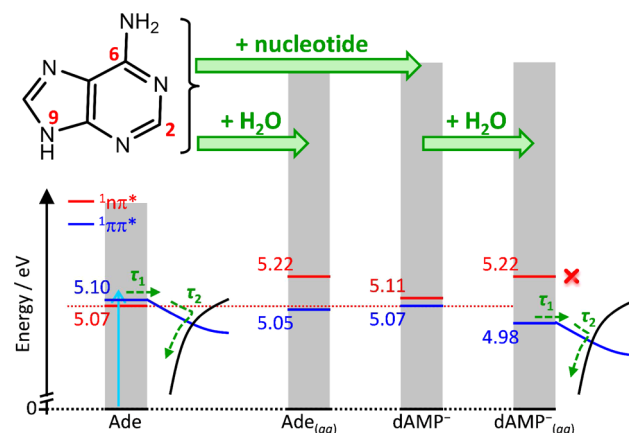


Figure 2. Variations in the calculated vertical excitation energies of Ade in various environments. The relative energies of the $^1n\pi^*$ and $^1\pi\pi^*$ states are indicated. The Franck–Condon region is shown as a gray shaded area. In differing environments, these change substantially, although the observed dynamics do not, which suggests that all dynamics are occurring along a single excited state and τ_1 is associated with motion away from the Franck–Condon region while τ_2 is associated with internal conversion to the ground state (black). Key atoms are labeled for Ade.

dynamics observed here for dAMP[−], suggesting that (i) the $^1\pi\sigma^*$ state is not involved in the decay of dAMP[−] following excitation at 4.66 eV and (ii) the dynamics of dAMP[−] are similar to those in Ade-9Me. The measured $\tau_2 = 1.1$ ps for Ade-9Me is, however, considerably longer than that observed here. This could be accounted for by the fact that those experiments were performed in a cold molecular beam as opposed to our ions, which are at room temperature or slightly higher. Under our conditions, the internal energy available in the ground state amounts to >0.46 eV. Hence, several low-frequency modes will be excited, and these can greatly accelerate excited-state dynamics. We note that Ade-9Me in aqueous solution has a τ_2 lifetime of 220 fs at 263 nm.³ It is of considerable interest to explore the effect of temperature on the excited-state dynamics in dAMP[−], and such experiments are currently being set up in our laboratory.

The sequential dynamics of Ade-9Me had been interpreted to proceed via a two-step model in which $i = 1$ and 2 were assigned to the $^1\pi\pi^* \rightarrow ^1n\pi^*$ and $^1n\pi^* \rightarrow S_0$ internal conversion processes, respectively.⁸ Several ab initio calculations have also been performed (see ref 12 and references therein). Although results depend critically on the level of theory, most recent studies indicate that the $^1n\pi^*$ state is not directly involved, contradicting the experimental interpretation.^{14,20} However, the situation is complicated by the prediction that the $^1n\pi^*$ and the $^1\pi\pi^*$ states become strongly mixed along the coordinates leading to two conical intersections.³¹ These involve puckering of the ring at either the C2 or C6 position, as labeled in Figure 2. A similar mechanism has been proposed for aqueous dAMP[−], for which there seems to be a general consensus.^{2,3,32} For aqueous Ade, theoretical studies suggest a slightly different mechanism because the strong vibronic coupling in the Franck–Condon regime leads to excitation of both $^1\pi\pi^*$ states and the low-lying $^1n\pi^*$ state.^{33,34} The first lifetime has been associated with decay from S_n to S_1 and the second with decay from the S_1 state. The geometry of the conical intersections was found to be similar between solution and the gas phase.³³

The dynamics of dAMP[−] have been measured by transient absorption and fluorescence up-conversion in aqueous solution by a number of groups,^{2,3,32} and recently, time-resolved photoelectron spectroscopy of solvated adenosine has been reported.³⁵ The most recent solution-phase measurements reported a biexponential decay with lifetimes of the slower ($i = 2$) component of $\tau_2 = 340$ fs for dAMP[−] (following excitation at 260 nm).³² Given the differences in environments and experimental techniques, the agreement of this time scale with our results is remarkable. It suggests that the charge localized on the phosphate, which is completely screened in solution,^{36,37} has little or no effect on the dynamics of the base in the gas phase. This is an important observation as it essentially allows us to view the charged phosphate as a spectator. It also suggests that the hydration of the nucleobase appears to have a small impact on the relaxation dynamics observed experimentally.

The above arguments lead us to conclude that the dynamics of the nucleobase appear to be relatively insensitive to the environment. However, what is the impact of the environment on the excited states, and can this provide any insight into the deactivation mechanism? To gain some insight into this question, we have performed TD-DFT calculations. Our choice of methodology is not to provide quantitative agreement with experiment, as there are much higher level calculations in the literature, but rather to gain insight into the *relative* changes between Ade in the differing environments. In Figure 2 (Table S1, Supporting Information), the energies of the relevant excited states are shown for Ade in isolation, water, a nucleotide, and an aqueous nucleotide. These trends are in agreement with high-level *ab initio* calculations.^{18,19,31,33}

Our calculations together with the available literature show that the energy of the $^1\pi\sigma^*$ state associated with the N9 position increases in energy in dAMP[−] relative to that in Ade and Ade-9Me, suggesting that this state is not involved in the decay of dAMP[−]. However, it is the relative ordering between the $^1\pi\pi^*$ to $^1n\pi^*$ states that is most revealing about the probable decay mechanism. With reference to Figure 2, in Ade, the $^1n\pi^*$ state lies below the $^1\pi\pi^*$ state, whereas in dAMP[−], this ordering is reversed. The effect of solvation is to increase the energy gap between the $^1\pi\pi^*$ and $^1n\pi^*$ states in dAMP[−]. One would anticipate that if the $^1n\pi^*$ state was an intermediate in the decay pathway, the presence of the sugar and phosphate and the effect of solvation on the dynamics would be marked. However, this is not the case. Hence, the dynamics in dAMP[−] appear not to involve the $^1n\pi^*$ state and are instead dominated by a $^1\pi\pi^* \rightarrow S_0$ internal conversion mechanism. This conclusion is in agreement with some theoretical studies that have stressed a similar independence on environment and a pathway dominated by the $^1\pi\pi^* \rightarrow S_0$ internal conversion mechanism.^{18,31} On the other hand, in solution, strong mixing of state character often prevents a strict diabatic label from being applied.³³ This makes definitive assignment of the mechanism difficult.

In our experiments on dAMP[−], we cannot determine the amount of mixing of the $^1n\pi^*$ state along the decay pathway, although it is worth noting that we observe no changes in the photoelectron anisotropy during the decay, which is consistent with dynamics occurring on a single excited state.²³ Our tentative conclusion that the dynamics do not directly involve the $^1n\pi^*$ state is consistent with those reached for solvated deoxyadenosine³¹ and with certain high-level calculations on solvated Ade;^{18,19} the biexponential dynamics observed are a consequence of motion away from the Franck–Condon region

toward conical intersections followed by internal conversion. We note that such biexponential decay has been observed in time-resolved photoelectron spectroscopy for dynamics that are occurring strictly on a single surface,³⁰ indicating that such data are not a prerequisite for the decay through multiple excited states. Finally, in our discussion above and in Figure 2, we have focused on the bright $^1\pi\pi^*$ state. There are in fact two close-lying $^1\pi\pi^*$ states in the relevant energy window (see the Supporting Information). However, when considering the other $^1\pi\pi^*$ state, the conclusion about the inactivity of the $^1n\pi^*$ state in the relaxation mechanism is not altered. Nevertheless, we note that, in principle, both $^1\pi\pi^*$ states can participate, especially in dAMP[−], where we have calculated the ordering between the two $^1\pi\pi^*$ states to change.

Above, we have shown the progression of the dynamics in going from isolated Ade through to dAMP[−] in aqueous solution. But how do these dynamics evolve in oligonucleotides? ESI provides a straightforward route to the generation of larger complexes in the gas phase, and we present studies on the dynamics of d(A)₂[−] and d(A)₃[−]. Their chemical structures are shown in Figure 1e and i, together with their time-resolved photoelectron spectra, Figure 1f and j, respectively. A similar analysis of the time-resolved spectra yielded lifetimes of $\tau_1 < 60$ fs and $\tau_2 = 340 \pm 90$ fs for d(A)₂[−] and $\tau_1 < 60$ fs and $\tau_2 = 380 \pm 120$ fs for d(A)₃[−]. The decay-associated spectra are shown in Figure 1h and l for d(A)₂[−] and d(A)₃[−], respectively.

Our results show that the ultrafast dynamics of the di- and trinucleotide are very similar to that of the mononucleotide (Figure 1a–d). Indeed, in aqueous solution, “monomer-like” dynamics have also been reported for d(A)_{*n*}[−] ($n \geq 2$). However, these were convoluted with the dynamics of much longer-lived excited states.^{38,39} Because of this, it has been difficult to exclusively identify the precise nature of these monomer-like dynamics in solution. It has been suggested that differences in the relaxation of a single Ade nucleobase in d(A)_{*n*}[−] relative to dAMP[−] may be caused by sterically hindered conformations or to adjacent bases evolving into the long-lived states.^{2,3,32} From our results on isolated oligonucleotides, the localized dynamics on the Ade base are only mildly influenced by the environment. There is a small increase in lifetime of 40–50 fs upon sequential addition of bases in the oligonucleotides. The spectral broadening observed between d(A)₂[−] and d(A)₃[−] can be correlated with the fact that the charged phosphate is on average farther away from one of the nucleobases (see Figure 1i), which will raise the vertical detachment energy and thus cause a red shift in the *eKE*. The maximum *eKE* remains the same because the other two bases are approximately at the same distance from the charge as in d(A)₂[−]. The observed decrease in the maximum *eKE* by ~ 0.2 eV for the oligonucleotides relative to dAMP[−] is likely a result of a more effective screening of the charge in the larger systems or may reflect interactions between the nucleobases.³⁶

In solution, additional long-lived dynamics (10s–100s ps) observed in transient absorption spectra of d(A)_{*n*}[−] ($n \geq 2$) have been assigned to the formation of excimer states that are delocalized over two (or more) adjacent π -stacked bases.^{2,3,38–40} In our data, no evidence for the formation of long-lived states, excimer or otherwise, has been observed. There may be several reasons for the lack of excimer dynamics observed. (i) The fraction of d(A)₂[−] or d(A)₃[−] that is in a stacked configuration is too low. Our experiments are performed with an internal energy of ~ 300 K, and the entropic cost for stacking is likely to be too high compared to the energy

gain from π -stacking. In solution, stacking is favored because of the unfavorable interaction of the nucleobase with water. The Bowers group has shown that only 65% of $d(A)_2^-$ was stacked at 80 K using ion mobility.⁴¹ (ii) It is also possible that excimer states are formed, but these cannot be observed due to our limited detachment window with the 3.1 eV probe pulses. However, time-resolved photoelectron spectroscopy on $(Ade)_2(H_2O)_3$ clusters would suggest that this is not a problem.⁴² Moreover, our data show a weak but discernible two-photon ionization peak, which has a combined probe energy exceeding the ionization energy of the base (see Figure S2 in the Supporting Information). (iii) Finally, it is plausible that a subpopulation of the ensemble is stacked but that the excimer states simply cannot form in the gas phase because of the nearby charge on the phosphate. Recent experiments on a dinucleotide containing Ade and thymine showed a clear signature of charge-transfer character of the long-lived state,⁴³ and this may be destabilized by the Coulomb interaction with an unscreened negative charge. For sufficiently large oligonucleotides or for water-clustered oligonucleotides, this possible destabilization would diminish.

■ ASSOCIATED CONTENT

■ Supporting Information

Analysis and residuals of global fitting. Comparison of Ade and $dAMP^-$ spectra. Theoretical details and results, including TD-DFT results and tables and calculated structures of Ade. This material is available free of charge via the Internet at <http://pubs.acs.org>.

■ AUTHOR INFORMATION

Corresponding Author

*E-mail: j.r.r.verlet@durham.ac.uk.

Present Addresses

[§]A.S.C.: Ultrafast X-ray Science Laboratory, Chemical Sciences Division, Lawrence Berkeley National Laboratory, Berkeley, California 94720, United States.

[†]G.M.R.: School of Chemistry, University of Bristol, Bristol BS8 1TS, United Kingdom.

Notes

The authors declare no competing financial interest.

■ ACKNOWLEDGMENTS

We are grateful to Prof. Martin Paterson (Heriot-Watt) for the use of his computing facilities. The project was funded by the Leverhulme Trust (F/00215/BH) and the EPSRC (EP/D073472/1). V.G.S. thanks the Royal Society for a University Research Fellowship. J.R.R.V. is grateful to the European Research Council for a Starting Grant (306536).

■ REFERENCES

- (1) Schreier, W. J.; Schrader, T. E.; Koller, F. O.; Gilch, P.; Crespo-Hernández, C. E.; Swaminathan, V. N.; Carell, T.; Zinth, W.; Kohler, B. Thymine Dimerization in DNA Is an Ultrafast Photoreaction. *Science* **2007**, *315*, 625–629.
- (2) Middleton, C. T.; de La Harpe, K.; Su, C.; Law, Y. K.; Crespo-Hernández, C. E.; Kohler, B. DNA Excited-State Dynamics: From Single Bases to the Double Helix. *Annu. Rev. Phys. Chem.* **2009**, *60*, 217–239.
- (3) Crespo-Hernández, C. E.; Cohen, B.; Hare, P. M.; Kohler, B. Ultrafast Excited-State Dynamics in Nucleic Acids. *Chem. Rev.* **2004**, *104*, 1977–2020.
- (4) Sagan, C. Ultraviolet Selection Pressure on the Earliest Organisms. *J. Theor. Biol.* **1973**, *39*, 195–200.
- (5) Ullrich, S.; Schultz, T.; Zgierski, M. Z.; Stolow, A. Direct Observation of Electronic Relaxation Dynamics in Adenine via Time-Resolved Photoelectron Spectroscopy. *J. Am. Chem. Soc.* **2004**, *126*, 2262–2263.
- (6) Canuel, C.; Mons, M.; Piuze, F.; Tardivel, B.; Dimicoli, I.; Elhanine, M. Excited States Dynamics of DNA and RNA Bases: Characterization of a Stepwise Deactivation Pathway in the Gas Phase. *J. Chem. Phys.* **2005**, *122*, 074316–074316.
- (7) Satzger, H.; Townsend, D.; Zgierski, M. Z.; Patchkovskii, S.; Ullrich, S.; Stolow, A. Primary Processes Underlying the Photostability of Isolated DNA Bases: Adenine. *Proc. Natl. Acad. Sci. U.S.A.* **2006**, *103*, 10196–10201.
- (8) Bisgaard, C. Z.; Satzger, H.; Ullrich, S.; Stolow, A. Excited-State Dynamics of Isolated DNA Bases: A Case Study of Adenine. *ChemPhysChem* **2009**, *10*, 101–110.
- (9) Wells, K. L.; Hadden, D. J.; Nix, M. G. D.; Stavros, V. G. Competing $\pi\sigma^*$ States in the Photodissociation of Adenine. *J. Phys. Chem. Lett.* **2010**, *1*, 993–996.
- (10) Kang, H.; Lee, K. T.; Jung, B.; Ko, Y. J.; Kim, S. K. Intrinsic Lifetimes of the Excited State of DNA and RNA Bases. *J. Am. Chem. Soc.* **2002**, *124*, 12958–12959.
- (11) Nix, M. G. D.; Devine, A. L.; Cronin, B.; Ashfold, M. N. R. Ultraviolet Photolysis of Adenine: Dissociation via the $^1\pi\sigma^*$ State. *J. Chem. Phys.* **2007**, *126*, 124312.
- (12) Kleinermanns, K.; Nachtigallová, D.; de Vries, M. S. Excited State Dynamics of DNA Bases. *Int. Rev. Phys. Chem.* **2013**, *32*, 308–342.
- (13) Serrano-Andrés, L.; Merchán, M.; Borin, A. C. Adenine and 2-Aminopurine: Paradigms of Modern Theoretical Photochemistry. *Proc. Natl. Acad. Sci. U.S.A.* **2006**, *103*, 8691–8696.
- (14) Barbatti, M.; Aquino, A. J. A.; Szymczak, J. J.; Nachtigallová, D.; Hobza, P.; Lischka, H. Relaxation Mechanisms of UV-Photoexcited DNA and RNA Nucleobases. *Proc. Natl. Acad. Sci. U.S.A.* **2010**, *107*, 21453–21458.
- (15) Barbatti, M.; Lischka, H. Nonadiabatic Deactivation of 9H-Adenine: A Comprehensive Picture Based on Mixed Quantum–Classical Dynamics. *J. Am. Chem. Soc.* **2008**, *130*, 6831–6839.
- (16) Barbatti, M.; Lan, Z.; Crespo-Otero, R.; Szymczak, J. J.; Lischka, H.; Thiel, W. Critical Appraisal of Excited State Nonadiabatic Dynamics Simulations of 9H-Adenine. *J. Chem. Phys.* **2012**, *137*, 22A503–514.
- (17) Serrano-Andrés, L.; Merchán, M. Are the Five Natural DNA/RNA Base Monomers a Good Choice from Natural Selection?: A Photochemical Perspective. *J. Photochem. Photobiol. C* **2009**, *10*, 21–32.
- (18) Ludwig, V.; da Costa, Z. M.; do Amaral, M. S.; Borin, A. C.; Canuto, S.; Serrano-Andrés, L. Photophysics and Photostability of Adenine in Aqueous Solution: A Theoretical Study. *Chem. Phys. Lett.* **2010**, *492*, 164–169.
- (19) Yamazaki, S.; Kato, S. Solvent Effect on Conical Intersections in Excited-State 9H-Adenine: Radiationless Decay Mechanism in Polar Solvent. *J. Am. Chem. Soc.* **2007**, *129*, 2901–2909.
- (20) Conti, I.; Garavelli, M.; Orlandi, G. Deciphering Low Energy Deactivation Channels in Adenine. *J. Am. Chem. Soc.* **2009**, *131*, 16108–16118.
- (21) Chen, J.; Thazhathveetil, A. K.; Lewis, F. D.; Kohler, B. Ultrafast Excited-State Dynamics in Hexaethyleneglycol-Linked DNA Homoduplexes Made of A-T Base Pairs. *J. Am. Chem. Soc.* **2013**, *135*, 10290–10293.
- (22) Horke, D. A.; Roberts, G. M.; Lecointre, J.; Verlet, J. R. R. Velocity-Map Imaging at Low Extraction Fields. *Rev. Sci. Instrum.* **2012**, *83*, 063101.
- (23) Lecointre, J.; Roberts, G. M.; Horke, D. A.; Verlet, J. R. R. Ultrafast Relaxation Dynamics Observed through Time-Resolved Photoelectron Angular Distributions. *J. Phys. Chem. A* **2010**, *114*, 11216.

- (24) Horke, D. A.; Verlet, J. R. R. Time-Resolved Photoelectron Imaging of the Chloranil Radical Anion: Ultrafast Relaxation of Electronically Excited Electron Acceptor States. *Phys. Chem. Chem. Phys.* **2011**, *13*, 19546–19552.
- (25) Eppink, A. T. J. B.; Parker, D. H. Velocity Map Imaging of Ions and Electrons Using Electrostatic Lenses: Application in Photoelectron and Photofragment Ion Imaging of Molecular Oxygen. *Rev. Sci. Instrum.* **1997**, *68*, 3477–3484.
- (26) Roberts, G. M.; Nixon, J. L.; Lecointre, J.; Wrede, E.; Verlet, J. R. R. Toward Real-Time Charged-Particle Image Reconstruction Using Polar Onion-Peeling. *Rev. Sci. Instrum.* **2009**, *80*, 053104.
- (27) Adamo, C.; Barone, V. Toward Reliable Density Functional Methods without Adjustable Parameters: The PBE0 Model. *J. Chem. Phys.* **1999**, *110*, 6158–6170.
- (28) Frisch, M. J.; Trucks, G. W.; Schlegel, H. B.; Scuseria, G. E.; Robb, M. A.; Cheeseman, J. R.; Scalmani, G.; Barone, V.; Mennucci, B.; Petersson, G. A.; Nakatsuji, H.; Caricato, M.; Li, X.; Hratchian, H. P.; Izmaylov, A. F.; Bloino, J.; Zheng, G.; Sonnenberg, J. L.; Hada, M.; Ehara, M.; Toyota, K.; Fukuda, R.; Hasegawa, J.; Ishida, M.; Nakajima, T.; Honda, Y.; Kitao, O.; Nakai, H.; Vreven, T.; Montgomery, J. A.; Peralta, J. E.; Ogliaro, F.; Bearpark, M.; Heyd, J. J.; Brothers, E.; Kudin, K. N.; Staroverov, V. N.; Kobayashi, R.; Normand, J.; Raghavachari, K.; Rendell, A.; Burant, J. C.; Iyengar, S. S.; Tomasi, J.; Cossi, M.; Rega, N.; Millam, J. M.; Klene, M.; Knox, J. E.; Cross, J. B.; Bakken, V.; Adamo, C.; Jaramillo, J.; Gomperts, R.; Stratmann, R. E.; Yazyev, O.; Austin, A. J.; Cammi, R.; Pomelli, C.; Ochterski, J. W.; Martin, R. L.; Morokuma, K.; Zakrzewski, V. G.; Voth, G. A.; Salvador, P.; Dannenberg, J. J.; Dapprich, S.; Daniels, A. D.; Farkas, Foresman, J. B.; Ortiz, J. V.; Cioslowski, J.; Fox, D. J. *Gaussian09*; Gaussian Inc.: Wallingford, CT, 2009.
- (29) Leang, S. S.; Zahariev, F.; Gordon, M. S. Benchmarking the Performance of Time-Dependent Density Functional Methods. *J. Chem. Phys.* **2012**, *136*, 104101–104112.
- (30) Mooney, C. R. S.; Horke, D. A.; Chatterley, A. S.; Simperler, A.; Fielding, H. H.; Verlet, J. R. R. Taking the Green Fluorescence out of the Protein: Dynamics of the Isolated GFP Chromophore Anion. *Chem. Sci.* **2013**, *4*, 921–927.
- (31) Gustavsson, T.; Sarkar, N.; Vaya, I.; Jimenez, M. C.; Markovitsi, D.; Improta, R. A Joint Experimental/Theoretical Study of the Ultrafast Excited State Deactivation of Deoxyadenosine and 9-Methyladenine in Water and Acetonitrile. *Photochem. Photobiol. Sci.* **2013**, *12*, 1375–1386.
- (32) Stuhldreier, M. C.; Temps, F. Ultrafast Photo-Initiated Molecular Quantum Dynamics in the DNA Dinucleotide D(ApG) Revealed by Broadband Transient Absorption Spectroscopy. *Faraday Discuss.* **2013**, *163*, 173–188.
- (33) Lan, Z.; Lu, Y.; Fabiano, E.; Thiel, W. QM/MM Nonadiabatic Decay Dynamics of 9H-Adenine in Aqueous Solution. *ChemPhysChem* **2011**, *12*, 1989–1998.
- (34) Mitrić, R.; Werner, U.; Wohlgemuth, M.; Seifert, G.; Bonačić-Koutecký, V. Nonadiabatic Dynamics within Time-Dependent Density Functional Tight Binding Method. *J. Phys. Chem. A* **2009**, *113*, 12700–12705.
- (35) Buchner, F.; Ritze, H.-H.; Lahl, J.; Lubcke, A. Time-Resolved Photoelectron Spectroscopy of Adenine and Adenosine in Aqueous Solution. *Phys. Chem. Chem. Phys.* **2013**, *15*, 11402–11408.
- (36) Chatterley, A. S.; Johns, A. S.; Stavros, V. G.; Verlet, J. R. R. Base-Specific Ionization of Deprotonated Nucleotides by Resonance Enhanced Two-Photon Detachment. *J. Phys. Chem. A* **2013**, *117*, 5299–5305.
- (37) Pluharova, E.; Schroeder, C.; Seidel, R.; Bradforth, S. E.; Winter, B.; Faubel, M.; Slavíček, P.; Jungwirth, P. Unexpectedly Small Effect of the DNA Environment on Vertical Ionization Energies of Aqueous Nucleobases. *J. Phys. Chem. Lett.* **2013**, *4*, 3766–3769.
- (38) Su, C.; Middleton, C. T.; Kohler, B. Base-Stacking Disorder and Excited-State Dynamics in Single-Stranded Adenine Homo-Oligonucleotides. *J. Phys. Chem. B* **2012**, *116*, 10266–10274.
- (39) Crespo-Hernandez, C. E.; Cohen, B.; Kohler, B. Base Stacking Controls Excited-State Dynamics in A-T DNA. *Nature* **2005**, *436*, 1141–1144.
- (40) Olaso-González, G.; Merchán, M.; Serrano-Andrés, L. The Role of Adenine Excimers in the Photophysics of Oligonucleotides. *J. Am. Chem. Soc.* **2009**, *131*, 4368–4377.
- (41) Gidden, J.; Bowers, M. T. Gas-Phase Conformational and Energetic Properties of Deprotonated Dinucleotides. *Eur. Phys. J. D* **2002**, *20*, 409–419.
- (42) Smith, V. R.; Samoylova, E.; Ritze, H. H.; Radloff, W.; Schultz, T. Excimer States in Microhydrated Adenine Clusters. *Phys. Chem. Chem. Phys.* **2010**, *12*, 9632–9636.
- (43) Doorley, G. W.; Wojdyla, M.; Watson, G. W.; Towrie, M.; Parker, A. W.; Kelly, J. M.; Quinn, S. J. Tracking DNA Excited States by Picosecond-Time-Resolved Infrared Spectroscopy: Signature Band for a Charge-Transfer Excited State in Stacked Adenine–Thymine Systems. *J. Phys. Chem. Lett.* **2013**, *4*, 2739–2744.